DISCOVERY

To Cite:
Oladele IO, Falana SO, Alatishe WA, Onuh LN, Adelani SO, Ajala OJ. Influence of weld joint design on mechanical and corrosion properties of welded dissimilar metals. *Discovery* 2023; 59: e122d1378
doi: https://doi.org/10.54905/disssi.v59i333.e122d1378

Author Affiliation:
[1]Department of Metallurgical and Materials Engineering, Federal University of Technology, Akure, PMB 704, Nigeria
[2]Centre for Nanomechanics and Tribocorrosion, School of Metallurgy, Chemical and Mining Engineering, University of Johannesburg, Johannesburg, South Africa
[3]Department of Material Science and Engineering, Katholieke Universiteit Leuven, Belgium
[4]Faculty of Materials and Chemical Engineering, University of Miskolc, Miskolc, Egyetem ut 1, 3515 Hungary, Budapest
[5]Materials Science and Engineering Program, University of Colorado Boulder, 80303, Colorado, USA

[*]**Corresponding author**
Department of Metallurgical and Materials Engineering, Federal University of Technology, Akure, PMB 704, Nigeria
E-mail: olumide706@gmail.com

ORCID List
Isiaka Oluwole Oladele 0000-0001-7168-1518
Samuel Olumide Falana 0000-00002-2938-0305

Peer-Review History
Received: 02 September 2023
Reviewed & Revised: 06/September/2023 to 13/November/2023
Accepted: 17 November 2023
Published: 21 November 2023

Peer-Review Model
External peer-review was done through double-blind method.

Discovery
pISSN 2278–5469; eISSN 2278–5450

Influence of weld joint design on mechanical and corrosion properties of welded dissimilar metals

Isiaka Oluwole Oladele[1,2], Samuel Olumide Falana[1*], Wasiu Agboladuro Alatishe[1,3], Linus Nnubuike Onuh[1,4], Samson Oluwagbenga Adelani[1,5], Oluwatosin Johnson Ajala[1]

ABSTRACT

This research study makes fundamental observations about dissimilar metal-welded joints, which combine mild steel and aluminum alloy plates, both 6 mm thick. We joined this metal using the shielded metal arc welding (SMAW) process with E308L-16 as the filler metal. We conducted welding on prepared double-V and butt joints and assessed mechanical properties through tensile, impact, and hardness tests. We examined microstructural characteristics using an optical microscope. To investigate the corrosion behavior, we immersed the welded joint in a 3.5 wt% NaCl solution and analyzed it using the potentiodynamic polarization electrochemical method. The results showed that dissimilar weld joints in the double-V configuration outperformed butt joints in tensile and hardness properties. Moreover, the double-V joint displayed more excellent thermodynamic stability in the 3.5 wt% NaCl solution compared to the commonly used butt joint. Consequently, the double-V joint design is the most suitable choice for achieving optimal mechanical and corrosion characteristics in these dissimilar weld joints for engineering applications.

Keywords: Butt joint, Double-V joint, shielded metal arc welding, dissimilar metals, mild steel, and aluminum.

1. INTRODUCTION

Among various manufacturing technologies, joining has been recognized as a crucial enabling technology for innovative and sustainable manufacturing. Functional requirements and technological constraints drive the need for some form of joining in the majority of products. Products usually consist of multiple components, and joining processes are fundamental to ensuring product functionality and enhancing manufacturing process efficiency (Martinsen et al., 2015). The prominent method of joining materials utilizes welding with metallic materials, fusing two or more parts by applying heat or pressure. This process extends beyond metals to everyday use with thermoplastics and, intriguingly, even wood (Sakthivel et al., 2020; Jamaludin et al., 2013; Arifin, 2020). Welding

DISCOVERY SCIENTIFIC SOCIETY

techniques categorize themselves based on the welding process employed, encompassing methods such as SMAW (arc welding with wrapped electrodes), SAW (submerged arc welding), GMAW (gas metal arc welding), GTAW (tungsten arc welding), and more.

Moreover, the classification of welding further distinguishes between welding similar materials (similar welding) and welding dissimilar materials (dissimilar welding) (Arifin, 2020). This categorization and the versatility of welding techniques establish it as a foundational technology in the manufacturing industry, enabling the creation of a wide array of products across diverse materials and applications. In modern times, integrating different materials has become essential in various industries, including power plants, petrochemical and chemical sectors, and construction. This need for material integration is particularly prominent in fabricating items like boilers, rig towers, and automotive components. The primary goal of joining dissimilar materials is to create an optimal material combination for a specific design that offers the desired mechanical properties, corrosion resistance, and cost-effectiveness (Musa et al., 2020).

Nevertheless, when it comes to welding dissimilar metals, achieving the same level of weld quality as with similar metals can be challenging. This challenge arises due to variations in the physical and chemical properties of the joined materials, even when welding conditions remain identical (Arifin, 2020; Touileb et al., 2022; Huang et al., 2022). Nonetheless, the objective of dissimilar welding is to harness the unique characteristics of different metals, ultimately reducing material costs and enhancing equipment reliability (Huang et al., 2022; Akkar and Alali, 2023). Research on dissimilar welding has a long history, focusing on joining various types of materials categorized into groups based on their ferrous or non-ferrous properties Thirunavukarasu et al., (2017), different steel classes Huang et al., (2022), Touileb et al., (2022), Oladele et al., (2018a), different aluminum classes El-Megharbel, (2018), Patel et al., (2019), steel with copper Shanjeevi et al., (2013), steel with aluminum Akkar and Alali, (2023), Sravanthi et al., (2019), and more.

Also, researchers have explored several methods for dissimilar metal joining, including Gas-Tungsten Arc Welding Sutrimo et al., (2019), Oladele et al., (2016), Shielded Metal Arc Welding, Friction Welding Attah et al., (2021), Oladele et al., (2016), and Laser Welding (Orishich et al., 2018). Dissimilar joints (DSJs) involving combinations of ferrous and non-ferrous metals hold significant practical appeal. There is a growing demand for such joints in various structural and industrial applications, driven by the need for cost-effective solutions while preserving material properties. Among dissimilar metal joints, those between aluminum and steel have received considerable attention (Gill and Pradhan, 2022; Thirunavukarasu et al., 2017; Oladele et al., 2018b). These aluminum-steel joints find extensive use in industries like automotive, marine, aerospace, and chemistry. Owing to technological advancements, their applications continue to expand. Aluminum-steel joints serve various purposes in automotive structures, including windscreen frames, bumper reinforcements, center pillars, and floor pans, with substantial potential for future growth.

Incorporating different Aluminum-Steel joints in a product offers several sustainable advantages. These include cost reduction by capitalizing on the price differences between the materials, weight reduction considering the differing densities, the combination of lightweight aluminum with high-strength steel, and the availability of hybrid properties (Mehta, 2019; Qin et al., 2022). However, welding dissimilar aluminum-steel materials is a complex process due to the intricate compatibility challenges during mixing. Aluminum and steel differ significantly in their melting temperatures, with aluminum at around 850 °C. Their ability to form oxides at distinct temperatures also varies. Aluminum (Al) exhibits a thermal expansion coefficient and specific heat nearly twice that of steel. Furthermore, aluminum's thermal conductivity is six times higher than steel's. In terms of elasticity, aluminum's modulus is three times that of steel; besides, aluminum and steel exhibit low solubility in each other (Mehta, 2019). An electrochemical difference of 1.22 volts between aluminum and steel further complicates the welding process.

These disparities in thermophysical, chemical, and mechanical properties pose several challenges, including the formation of intermetallic compounds (IMCs), the presence of a heat-affected zone (HAZ), metallurgical precipitation, defects, distortion, and reduced mechanical joint properties (Mehta, 2019; Gill and Pradhan, 2022; Newishy et al., 2023). Hence, understanding how to use these essential materials for various engineering applications effectively has become a critical area of investigation. Numerous researchers have delved into various welding processes for joining dissimilar metals while examining their mechanical, corrosion, and other relevant properties. Additionally, they have considered the type of joint used, whether it is a lap or butt joint, accounting for the disparities between the two materials. For instance, Qin et al., (2022) studied the microstructure and mechanical properties of aluminum alloy/stainless steel dissimilar ring joints using inertia friction welding. This welding process exhibited a significant coupling effect between thermal and mechanical aspects.

Consequently, the thermo-mechanically affected zone (TMAZ) on the aluminum side underwent inadequate recrystallization, resulting in zonal features. The TMAZ regions showed distinct differences in crystal orientation and grain size. The rapid cooling rate hindered the growth of intermetallic compounds (IMCs) on the joint faying surface. The metallurgical bonding characteristics

varied due to the discontinuous distribution of IMCs. The average tensile strength reached 161.3 MPa, equivalent to 92.2% of the strength of 2219-O. The fracture occurred in the base metal on the aluminum side, displaying ductile fracture characteristics. In a separate study, Newishy et al., (2023) investigated friction stir welding of dissimilar materials: Al 6061-T6 and AISI 316 stainless steel. Dissimilar butt joints were formed between these materials using different processing parameters. Electron backscatter diffraction (EBSD) analysis revealed significant continuous dynamic recrystallization (CDRX) in the stir zone (SZ) of the aluminum side, mainly comprising weaker aluminum along with steel fragments.

The steel experienced severe deformation and discontinuous dynamic recrystallization (DDRX). Increasing rotation speed during friction stir welding (FSW) enhanced the ultimate tensile strength (UTS). Irrespective of the specimen, tensile failure occurred at the SZ on the aluminum side. The collective findings of various researchers have observed that failures in aluminum and steel joints typically occur on the aluminum side due to their lower strength. Therefore, further investigation into parameters like weld joint design is crucial to understanding the strength and failure modes of such joints. There is a need to enhance the strength characteristics of these joints on the aluminum end.

The current study aims to examine the mechanical and corrosion characteristics of dissimilar metals, specifically aluminum and mild steel, using the shielded metal arc welding (SMAW) technique, considering both double-V and butt joints. SMAW, also known as Shielded Metal Arc Welding, is a widely used welding method in various industrial applications. This technique involves metal electrode wires coated with flux. The welder uses an arc to join a covered electrode with a weld pool. As the welder introduces the coated electrode into the welding pool, the coating decomposes, producing gases that shield the pool. This process does not require pressure and uses the metal filler from the electrode, contributing to metal deposits for joining metals and applying a metal surface to products (Arifin, 2020).

2. MATERIALS AND METHODS

Materials

For this investigation, we utilized mild steel sheets compliant with ASME CODE SA-516, a standard specification for pressure vessel plates suitable for moderate- and lower-temperature services. Additionally, we used aluminum alloy sheets (Al5052) as the second base material. We procured these materials from a local supplier in Akure, Ondo State, Nigeria. We used a stainless-steel electrode with the code name E308L-16 as the filler metal in our welding process. This electrode features a rutile-basic coating explicitly designed for welding ASTM 304L base materials for low-temperature applications. We acquired this electrode from a local vendor in Akure, Ondo State, Nigeria, just like the base materials. The chemical composition of each material is in Tables 1 and 2, and the chemical composition of the stainless-steel electrode used in our welding work is in (Table 3).

Table 1 Mild Steel Chemical composition

Elements	Fe	C	Si	Mn	P	S	Ni	Cr	Mo	N	Cu	Others
Percentage (%)	98.354	0.071	0.327	0.546	0.004	0.003	0.051	0.027	0.013	0.008	0.022	0.594

Table 2 Aluminum alloy (Al5052) Chemical composition

Element	Al	Si	Fe	Cu	Mn	Mg	Zn	Cr	Others
Percentage (%)	97.7	0.25	0.4	0.1	0.1	2.8	0.1	0.35	0.15

Table 3 Electrode Chemical composition

Element	Fe	C	Mn	Si	Cr	Ni
E308L-16	69.875	0.025	1	0.60	18.5	10

Welding and Sample Preparation

The aluminum and mild steel sheets were cut into 60 x 80 mm pieces using a cutting machine equipped with a 4 1/2 - inch carbon cutting disc. In total, we prepared four plates, with two plates from each material. We then used a grinding machine with a four-1/2-inch carbon grinding disc to bevel one side of each plate to an angle of less than 3 mm. To create a double-V shape, we placed the prepared beveled pieces, one from aluminum and one from mild steel, adjacent. We repeated the same process for the remaining un-beveled pieces, forming butt joints.

The welding process was the Shielded Metal Arc Welding (SMAW) technique, following the specified requirements in (Table 4). After completing the welding, we extracted dumbbell-shaped samples from both the welded joints and the base metals for tensile

strength testing. We also performed additional machining to facilitate hardness testing and acquire microstructural samples. These samples were separated into three sections: base metal (BM), heat-affected zone (HAZ), and weld metal (WM).

Table 4 Welding Processes.

Type of joint	Plate thickness	Electrode Diameter (mm)	Time (sec)	Amperage Range (*I*)	No of Passes
Double-V	6 mm	3.25	32.7	95 – 125	3
Butt	6 mm	3.25	32.5	95 – 125	3

Evaluation and characterization of the welded sample

Tensile Test

Tensile test specimens are following the (ASTM A370-08A, 2008) standards. We conducted the tests using a Su Zhou Long Sheng universal testing machine. The machine applied a load of 300 KN to each specimen at a crosshead velocity of 5 mm/min, resulting in an initial strain rate of 0.98 s-1. We securely clamped the specimen at both ends using the machine's grips. The tensile testing equipment uniformly stretched the specimen while continuously measuring the applied load and elongation. Due to the applied load, each sample underwent permanent deformation and eventually fractured, resulting in the separation of the specimen into two distinct parts (Oladele et al., 2018b).

Hardness Test

Hardness assessment followed the Brinell hardness testing methodology, employing a load increment of Hardness Brinell Wolfram carbide (HBW) 5/250. We subsequently examined the hardness of the specimens, commencing at the fusion zone of the welded plates while also encompassing the corresponding section of the base metals to facilitate a comparative analysis of the findings. The indenter, in the form of a steel ball, was forcibly applied to the test material. The resulting indentation diameter (d) was duly measured, thereby enabling the calculation of the projected area and the subsequent determination of the material's hardness.

Impact Test

The impact tests were conducted on four samples, namely the base metals (aluminum and mild steel) and the welded samples (the butt and the double-V joint), in order to ascertain the impact strengths using the "V-notch method employing the Honfield Balance Impact Testing Machine". Prior to the installation of the machine, we notched a v-shaped edge on the test samples to a depth of 2mm using a hand file. Subsequently, we attached the notched test sample to the impact testing machine, and we activated the machine to apply a constant impact force to the test sample. We determined the impact strength by reading the calibrated scale on the impact testing machine, which quantifies the amount of impact energy absorbed by the specimen before yielding.

Metallographic Examination

The specimens were subjected to grinding using various grades of emery paper (220, 320, 500, 600, 800, and 1000), followed by polishing and etching for approximately 30 seconds using the corresponding etchants as outlined in (Table 5). Using a Nikon Optiphot metallurgical microscope and a Nikon D70 digital camera with magnifications of 50 and 100, we captured the micrographs of the samples. Optical microscopy was employed to examine the microstructures of the weld zone (WZ), heat-affected zone (HAZ), and parent metal (PM).

Table 5 Etchant for respective metal.

Metal	Etchant
Mild steel	2% Nitric acid
Aluminium	Highly diluted acid
Stainless steel	3% Nitric acid, 100% ethanol, 20cm3 HCl

Corrosion Test

We conducted potentiodynamic polarization and open circuit potential (OCP) measurements using the AUTOLAB PGSTAT 204N instrument. We performed the electrochemical investigations using a three-electrode cell configuration at ambient temperature. We used carbon steel as the working electrode, with a geometric area of 1 cm2 embedded in resins. We used platinum as the counter electrode and a silver/silver chloride reference electrode. The electrolyte was NaCl (sea water), with a weight percentage of 3.5%.

We conducted the linear polarization analysis within a potential range of -250 mV to +250 mV, with a scan rate of 1.0 mVs-1; this allowed us to determine the current density (Icorr), corrosion rate, and anodic tafel slope (Ba). We performed the abovementioned process on the weld and heat-affected zones (HAZs) of equal sizes of (10 x 10) mm each. Oladele et al., (2018a) also carried out a similar procedure.

3. RESULTS AND DISCUSSION

Tensile Properties

We assessed the tensile characteristics, including the ultimate tensile strength, tensile modulus, and maximum strain. The mean values in Figures 1–4 represent the data we collected from the measurements. The analysis presented in Figure 1 unveiled that, in terms of tensile properties, mild steel exhibited superiority over aluminum among the base materials employed, having an ultimate tensile strength of 464.24 MPa compared to 412.25 MPa of the aluminum alloy, as seen in (Figure 2). This discrepancy can be due to the inherent characteristics of mild steel, including its density, grain structure, atomic structure, and the alloying elements it encompasses. Moreover, we observed that the double-V joint of the welded component demonstrated superior tensile properties encompassing ultimate tensile strength, maximum strain, and tensile modulus in comparison to the butt joint of the welded component.

This enhancement can be due to the formation of intermetallic compounds between the two base metals and the proper filling strengthening mechanism made possible by the weld joint design. The intermetallic compounds result from the interaction between mild steel, aluminum, and the filler metal, leading to the creation of a phase that possesses greater strength than the parent metal (Oladele et al., 2018b). Also, using a double-V joint allows for the load distribution across two separate weld beads on either side of the joint. This distribution of load minimizes stress concentration at any specific point, thereby reducing the susceptibility of the joint to failure under tensile loads. Conversely, in a typical butt joint, the entire load is concentrated on a single weld bead at the center of the joint.

This load concentration can result in stress concentration and potentially give rise to welding defects or failures, particularly when subjected to high tensile loading. Likewise, from Figure 3, the double-V joint exhibited a higher maximum strain than the butt joint but slightly lower than that of the base metals. In contrast, in Figure 4, the double-V joint exhibited a higher tensile modulus than the other joint type employed and the base metal aluminum alloy 5052 but lower than the mild steel base metal; this can also be because of the presence of intermetallic phases formed during the welding process between the electrode used and the base metals. These results were in agreement with the work of (Brajesh et al., 2015).

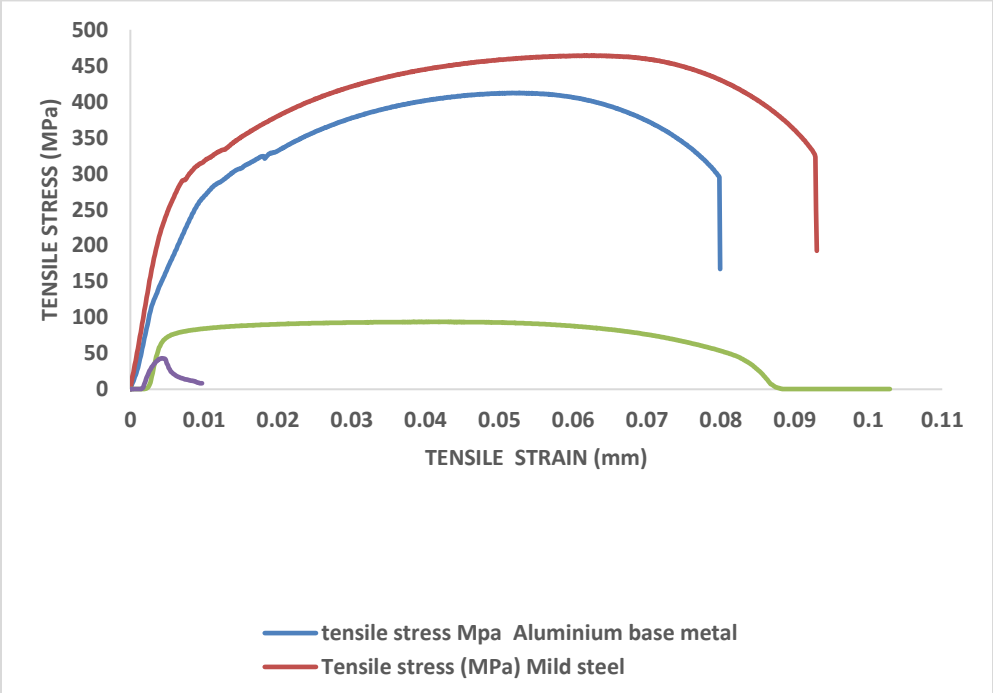

Figure 1 Stress-strain curve of the base metals and weld joints.

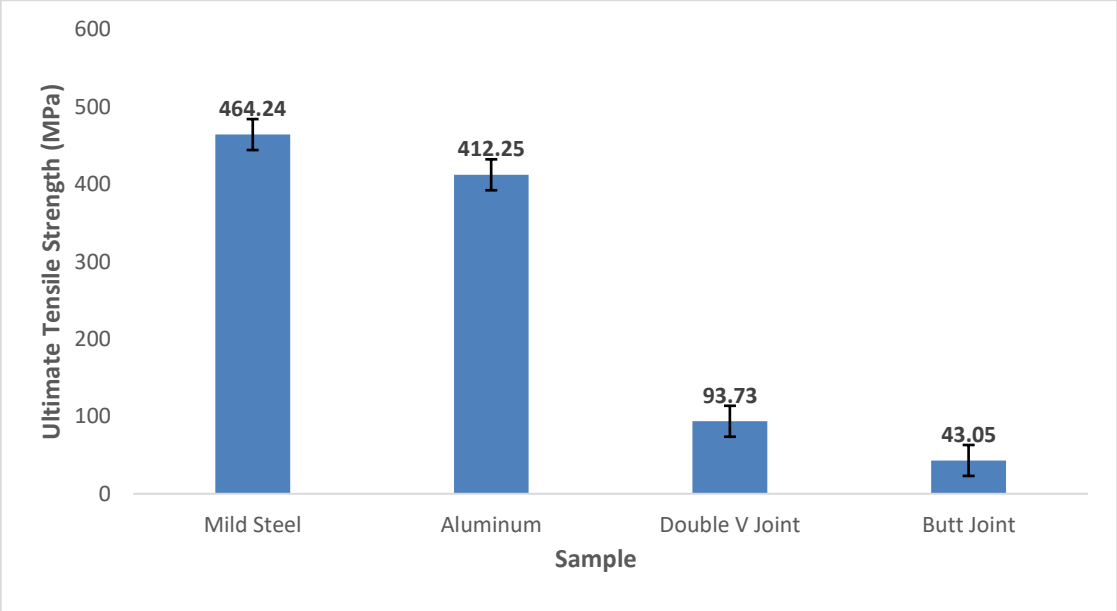

Figure 2 Ultimate tensile strength of the base metals and weld joints.

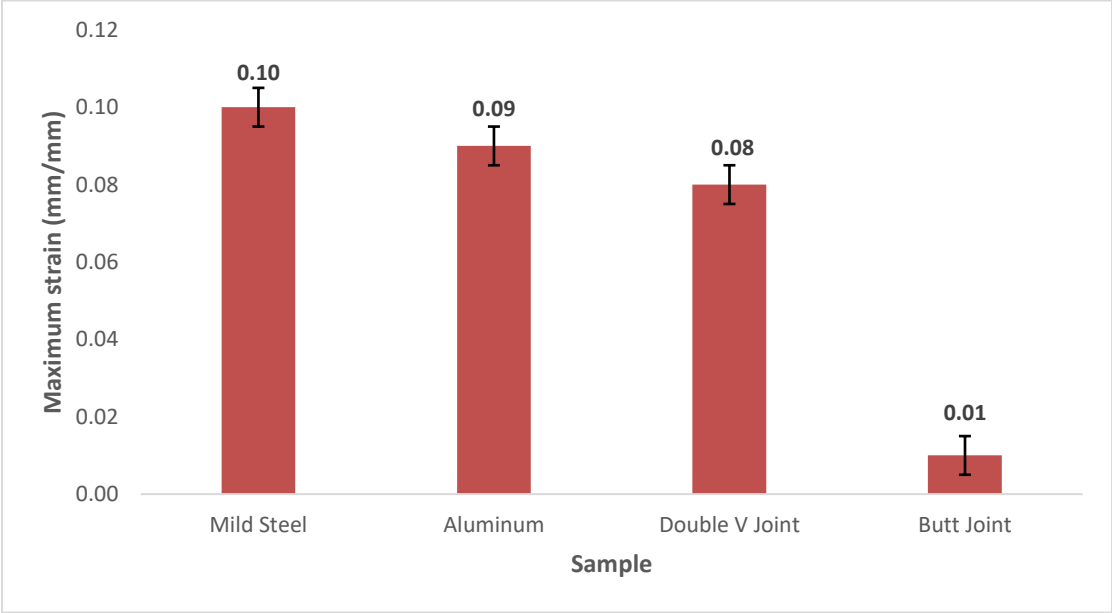

Figure 3 Maximum strain of the base metals and weld joints.

Hardness Property

The hardness values of the base metals and welded components is presented in (Figure 5). From Figure 5, we observed that the base metal from mild steel exhibited the highest hardness of 142.89 HBR, followed by the double-V joint with a hardness of 109.4 HBR and the butt joint with a hardness of 97.5 HBR. Conversely, the aluminum base metal demonstrated the lowest hardness value of 64.59 HBR. Thus, an enhancement of 69% was noted between the double-V joint and aluminum base metal, while we observed a 51% enhancement between the butt joint and aluminum base metal. This enhancement can be attributed to the diffusion of alloying elements in the weld pool, resulting in the formation of distinct phases from the base metals and ultimately affecting the mechanical properties. The dissimilar metal-welded samples exhibited intermediate strength and hardness values between mild steel and aluminum. Fusing these two dissimilar metals could be a viable fabrication method for applications requiring structural properties with specific hardness, considering environmental and cost factors. Figure 5 also shows that the double-V welded joint is superior to the butt welded joint, which is consistent with (Brajesh et al., 2015).

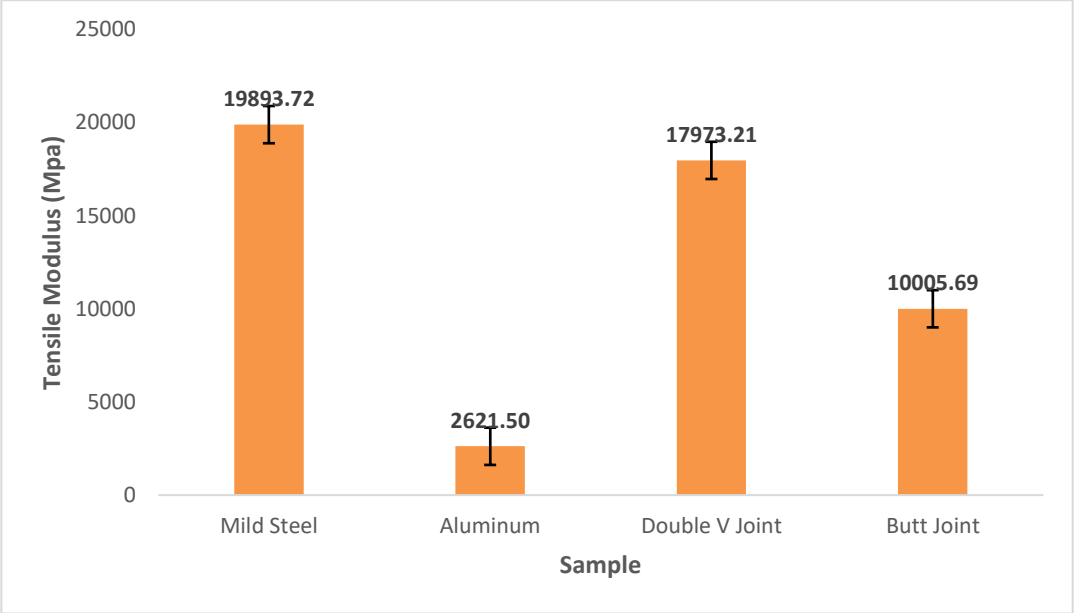

Figure 4 Tensile Modulus of the base metals and weld joints.

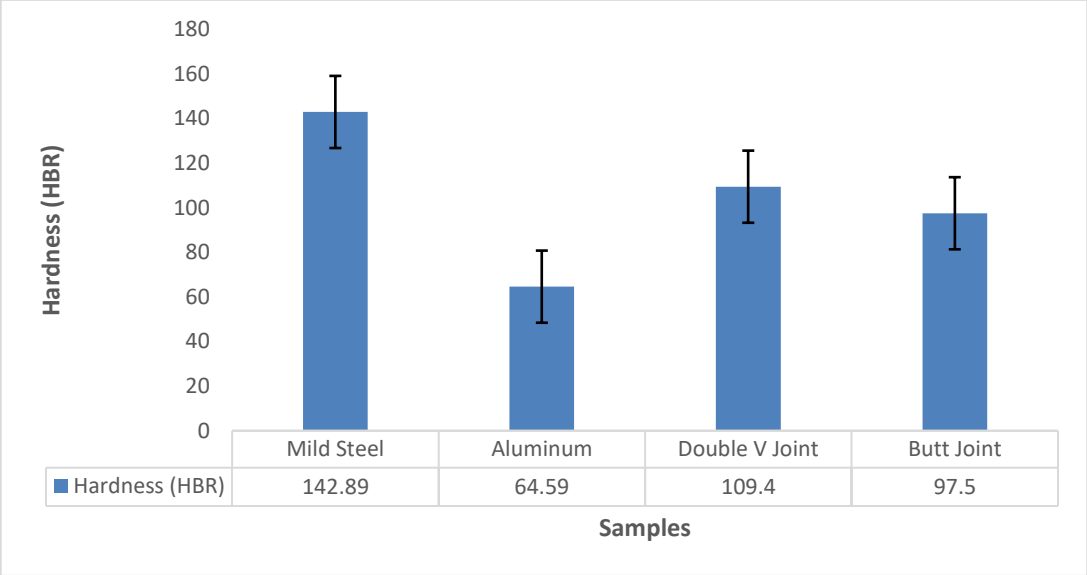

Figure 5 Hardness (HBR) of the base metals and weld joints.

Impact Property

Figure 6 illustrates the measured impact energy in joules for both the base metal and the welded component. We observed that the base metals exhibited higher impact energy than the welded samples. Specifically, mild steel demonstrated the highest impact energy at 62.37 J, while the butt joint displayed the lowest impact energy at 13.23 J. This discrepancy can be because of the inherent challenges associated with welding dissimilar metals, namely their varying melting points, thermal conductivities, and expansion coefficients. Consequently, these differences can result in welding flaws such as cracking and porosity, ultimately diminishing the overall impact strength. Moreover, we noticed that the double-V joint exhibited tremendous impact energy when compared to the butt joint; this can be due to the double-V joint possessing a larger cross-sectional area. Consequently, the stress is distributed over a larger surface area, reducing the likelihood of failure under impact loading.

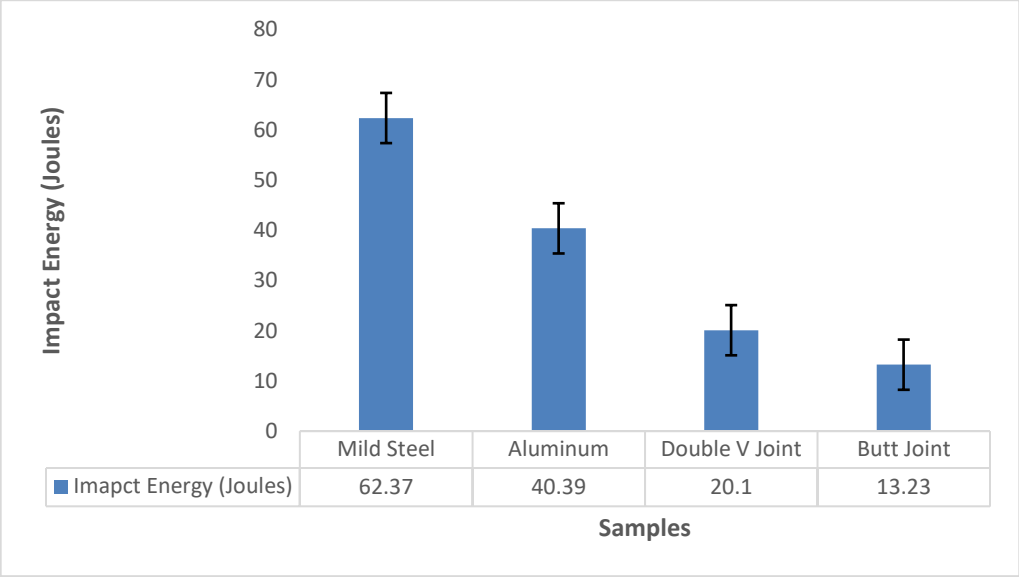

Figure 6 Impact Energy of the base metals and weld joints.

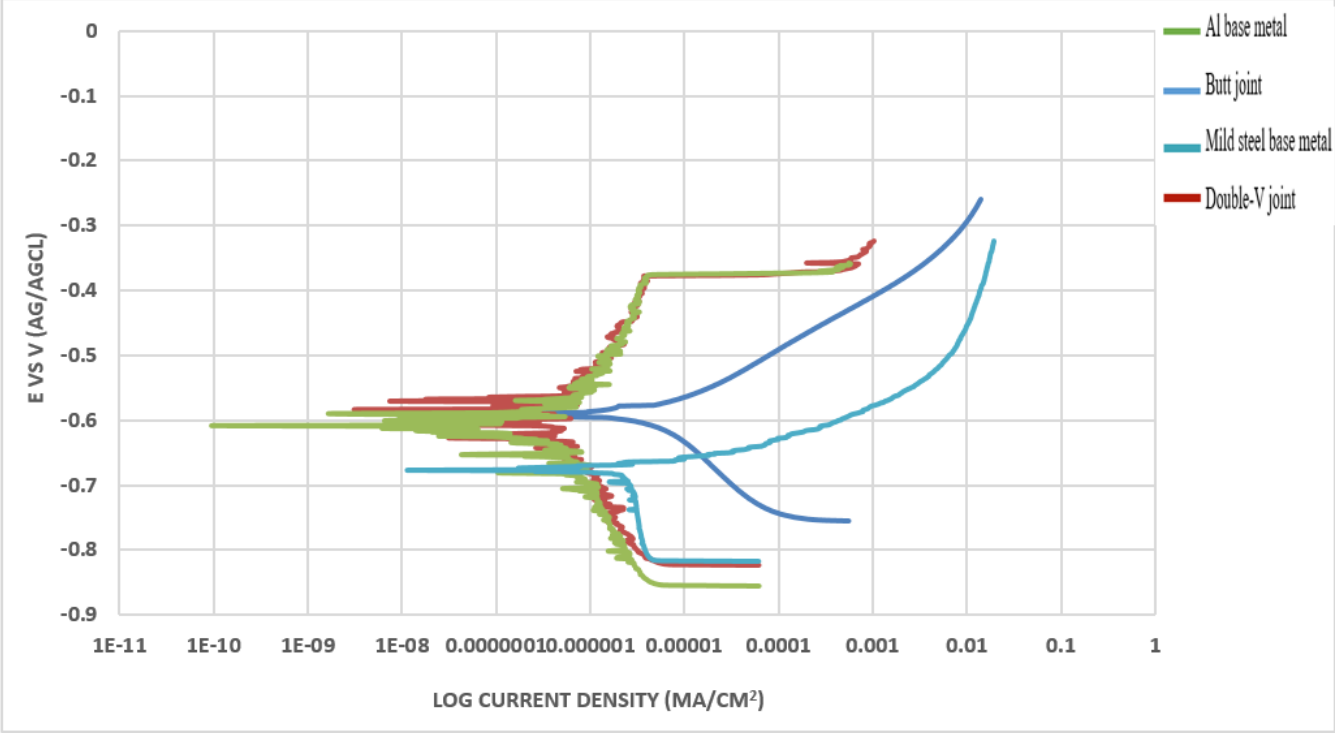

Figure 7 Potentiodynamic polarization curves of the base metals and the welded joints samples in the 3.5 wt% NaCl solution

Corrosion Properties

The potentiodynamic polarization curves of the base metals and the welded joint, which consists of the weld zone and the base metals, were examined in a 3.5 wt% NaCl solution (saline environment), as depicted in (Figure 7). Meanwhile, Figure 8 provides the corrosion rate for each material. Notably, the samples displayed diverse polarization and passivity characteristics, as indicated by the distinct corrosion rate values in (Figures 7 and 8). The results revealed that aluminum exhibited a lower corrosion rate than mild steel among the base metals. This disparity can be due to the inherent corrosion resistance of aluminum relative to steel.

Regarding the welded samples, we also observed that the double-V joint displayed a lower corrosion rate compared to the butt joint. This discrepancy arises from the larger surface area exposed to the corrosive environment in the butt joint, rendering it more susceptible to cracking than the V-joint. Overall, both welded samples exhibited a higher corrosion rate than the base metals, as evident in Figure 8; this can be because of the formation of intermetallic compounds (IMCs) at the weldment interface. These IMCs

are brittle and possess poor corrosion resistance, rendering the weldment more vulnerable to corrosion than the base metals. Furthermore, the welding process may introduce defects in the weldment, such as porosity and cracking, which can serve as initiation sites for corrosion.

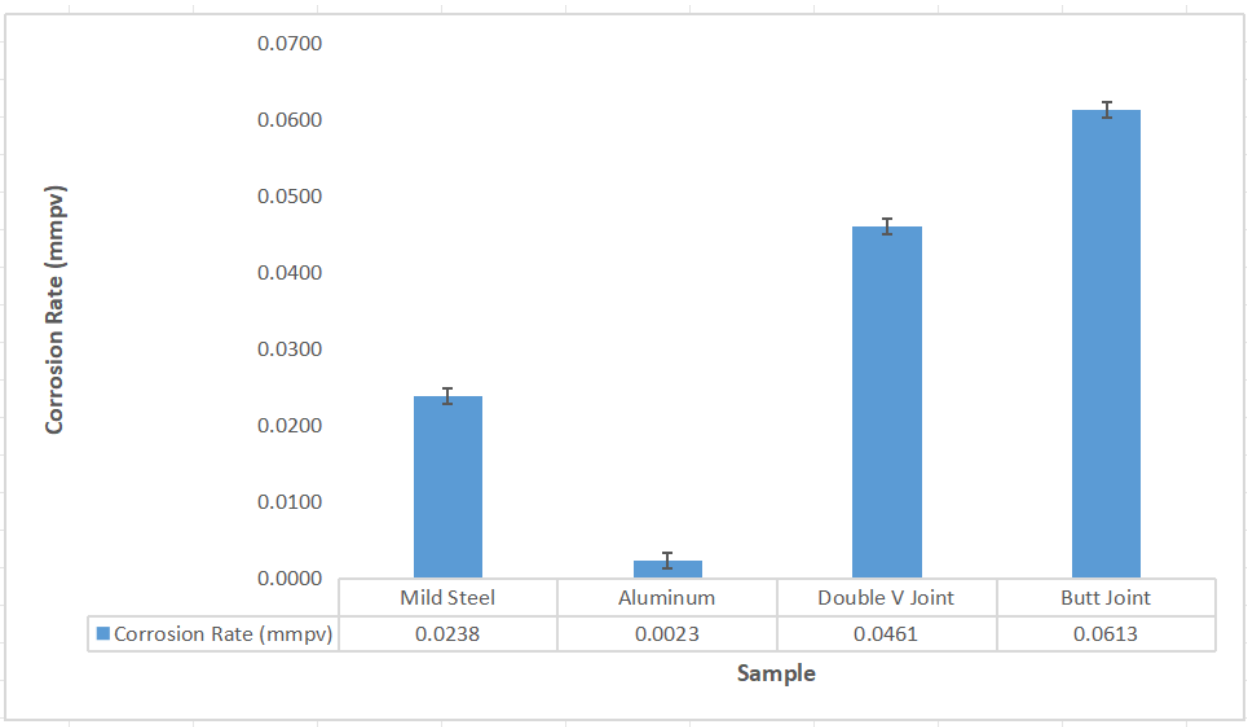

Figure 8 Corrosion rate of base metals and the welded joints

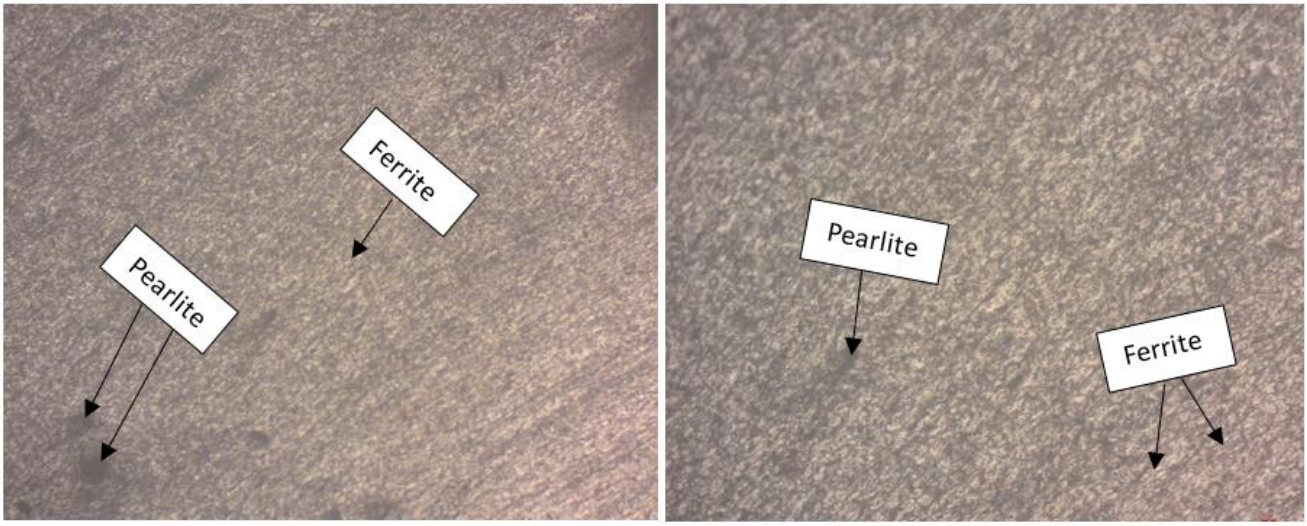

Figure 9a Microstructure analysis of Mild steel (Base metal).

Metallographic Microstructural Analysis

The examination of the microstructure is evident in (Figures 9–11). It was noted in Figure 9a that the microstructural analysis of the mild steel displayed a heterogeneous composition consisting of both ferrite and pearlite phases. The dark spots represent the pearlite phase, while the bright spots signify the presence of the ferrite phase. Additionally, we observed that the pearlite phases, both globular and laminar, were dispersed throughout the ferrite phase. Figure 9b delineates the microstructure of the aluminum 5052 alloy base metal. The micrograph revealed the formation of aluminum oxide (Al2O3) on the surface, which covers the entirety of the aluminum. Furthermore, we observed fine β-AlMg precipitates distributed throughout the entire matrix. Sravanthi et al., (2019) observed similar results.

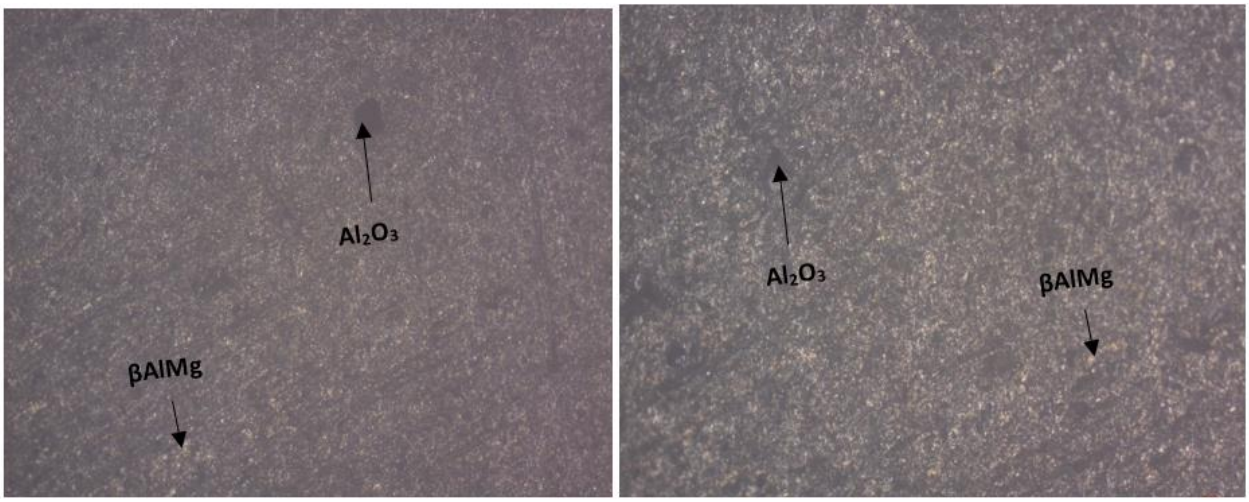

Figure 9b Microstructure analysis of Aluminum 5052 alloy (Base metal).

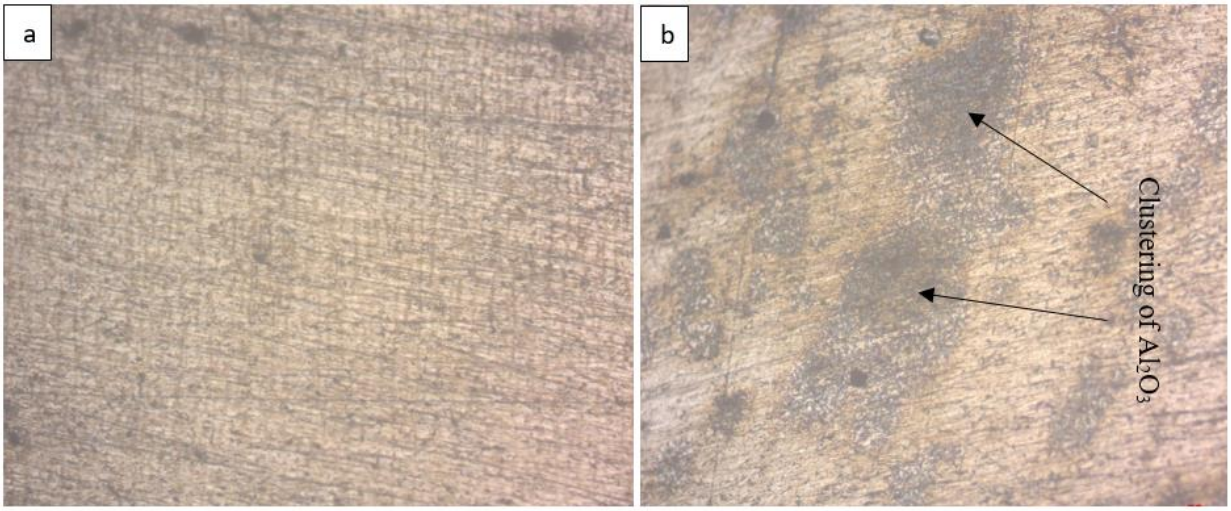

Figure 10 Heat affected zone (HAZ) of (a): Mild steel. (b): Aluminum alloy

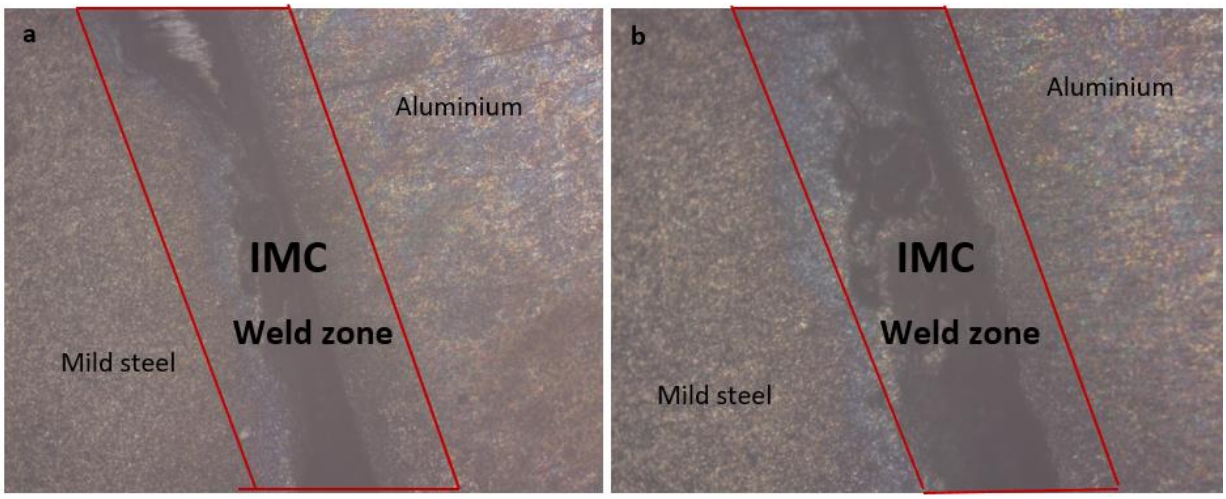

Figure 11 Aluminium-mild steel (a) double-v joint. (b) Butt joint

Figure 10 shows the heat-affected zone (HAZ) of the base metals. The micrograph in Figure 10a reveals that the ferrite distribution is more significant than the pearlite distribution. The heat generated during welding causes recrystallization, which disperses some coagulated pearlite within the ferrite phase, but not to the same extent as in the base metal. A similar result was also

observed in Oladele et al., (2018b) when a comparative investigation of the mechanical properties and corrosion behavior of dissimilar metals (austenitic stainless steel and mild steel) weld fusion zones, heat-affected zones, and base metals. However, a dark spot was observed on the surface of the base metal in the heat-affected zone (HAZ) in (Figure 10b). This observation indicates the clustering of Al2O3 due to the heat generated during the welding process for both base metals.

Additionally, Figure 11 illustrates the micrographs of the double-v and butt joints of the base metals. We noticed an intermetallic compound at the weld zone of both joint types due to the heat generated while welding the metals together. The intermetallic compound formed in the double-v joint will disperse appropriately due to the welding area of the joint. On the other hand, butt joints can occasionally create stress concentration points at the center of the joint due to the sudden change in material thickness. In contrast, double-V joints exhibit a more gradual transition from the base materials to the groove, thereby reducing stress concentrations that can lead to a decrease in the properties of the welded material.

4. CONCLUSION

The purpose of this study was to investigate the mechanical and corrosion properties of dissimilar metals, namely aluminum and mild steel, through the utilization of shielded metal arc welding. Two types of joints, specifically the double- V and butt joint, were employed in the welding process. Based on the results, we strongly advised that the double-V welding joint be implemented instead of the butt-end joint. This recommendation stems from the fact that the double-V joint exhibited superior performance in terms of mechanical properties when compared to the butt joint. Furthermore, the double-V welded joint demonstrated a lower corrosion rate in comparison to the butt welded joint. This characteristic renders the double-v joint more desirable, particularly in environments with high salinity.

Acknowledgement

We thank the participants who all contributed samples to the study and the welding workshop of the Department of Metallurgical and Materials Engineering at the Federal University of Technology Akure, Nigeria.

Author's Contribution

Name	Contribution
Isiaka Oluwole Oladele	Review manuscript and approve the version to be published.
Samuel Olumide Falana	Acquisition and analysis of data. Drafting the Manuscript
Wasiu Agboladuro Alatishe	Substantial contribution to the acquisition of data and analysis of data
Linus Nnabuike Onuh	Substantial contribution to drafting the manuscript
Samson Oluwagbenga Adelani	Review of manuscript to be sent out for publication
Oluwatosin Johnson Ajala	Editing of manuscript to journal format.

Informed consent: Not applicable.

Ethical approval: Not applicable.

Conflicts of interests: The authors declare that there are no conflicts of interests.

Funding: The study has not received any external funding.

Data and materials availability

All data associated with this study are present in the paper.

REFERENCES AND NOTES

1. Akkar AY, Alali M. Resistance Spot Welding of Dissimilar Metals AISI 1006 Low Carbon Steel and AA6061 Aluminum Alloy Using Zinc and Tin Coating. Kufa J Eng 2023; 14(3):1-16. doi: 10.30572/2018/KJE/140301

2. Arifin A. Dissimilar metal welding using shielded metal arc welding: A Review. Technol Rep Kansai Univ 2020; 62(4):1935–1948.
3. ASTM A370-08A. Standard Test Methods and Definitions for Mechanical Testing of Steel Products. ASTM Int 2008.
4. Attah BI, Lawal SA, Akinlabi ET, Bala KC. Evaluation of mechanical properties of dissimilar aluminium alloys during friction stir welding using tapered tool. Cogent Eng 2021; 8(1):1909520. doi: 10.1080/23311916.2021.1909520
5. Brajesh KS, Jha AK, Pravin SK. Effects of Joint Geometries on Welding of Mild Steel by Shielded Metal Arc Welding (SMAW). Int Res J Eng Technol 2015; 2(7):95-100.
6. El-Megharbel HAE-HA. Friction stir welding of dissimilar aluminum alloys. World J Eng Technol 2018; 6:408-419. doi: 10.4236/wjet.2018.62025
7. Gill D, Pradhan MK. A Review on Advances in Friction Welding of Dissimilar Metals. Lect Notes in Mech Eng 2022; 38:181–197. doi: 10.1007/978-981-19-0676-3_15
8. Huang CH, Hou CH, Hsieh TS, Tsai L, Chiang CC. Investigation of distinct welding parameters on mechanical and corrosion properties of dissimilar welded joints between stainless steel and low carbon steel. Sci Prog 2022; 105(4):368504221126795. doi: 10.1177/00368504221126795
9. Jamaludin SB, Mazlee MN, Kadir SKA, Ahmad KR. Mechanical properties of dissimilar welds between stainless steel and mild steel. Adv Mat Res 2013; 795:74–77. doi: 10.4028/www.scientific.net/AMR.795.74
10. Martinsen K, Hu SJ, Carlson BE. Joining of dissimilar materials. CIRP Ann Manuf Technol 2015; 64(2):679–699. doi: 10.1016/j.cirp.2015.05.006
11. Mehta KP. A review on friction-based joining of dissimilar aluminum-steel joints. J Mater Res 2019; 34:78–96. doi: 10.1557/jmr.2018.332
12. Musa AA, Dauda ET, Bello KA, Adams SM. Optimization of TIG Welding Parameters on the Tensile Strength Performance of Ferritic Stainless Steel Welds Using Response Surface Methodology. Indian Journal of Engineering 2020; 17(48):591-604
13. Newishy M, Jaskari M, Järvenpää A, Fujii H, Abdel-Aleem HA. Friction Stir Welding of Dissimilar Al 6061-T6 to AISI 316 Stainless Steel: Microstructure and Mechanical Properties. Materials (Basel) 2023; 16(11):4085. doi: 10.3390/ma16114085
14. Oladele IO, Agbabiaka OG, Yakubu NA. Influence of Welding Process and Thickness on the Mechanical Properties of SA516 Steel. JAPETT 2016; 44:11–16. doi: 10.13140/RG.2.2.12729.60009
15. Oladele IO, Betiku OT, Okoro AM, Eghonghon O, Saliu LO. Comparative Investigation of the Mechanical Properties and Corrosion Behavior of Dissimilar Metal Weld Fusion Zone, Heat Affected Zones and Base Metals. Ann Fac Eng Hunedoara 2018b; 16:187–192.
16. Oladele IO, Betiku OT, Okoro AM, Eghonghon O. Microstructure and Mechanical Properties of 304L and Mild Steel Plates Dissimilar Metal Weld Joint. Acta Tech Corvin Bull Eng 2018a; 11(2):77–81.
17. Orishich A, Malikov A, Karpov E. Analysis of the effect of the thermomechanical processing on the laser weld joint of aluminum alloys of Al-Mg-Li and Al-Cu-Li. Procedia CIRP 2018; 74:442–445. doi: 10.1016/j.procir.2018.08.162
18. Patel V, Li W, Wang G, Wang F, Vairis A, Niu P. Friction stir welding of dissimilar aluminum alloy combinations: State-of-the-art. Metals 2019; 9(3):270. doi: 10.3390/met9030270
19. Qin F, Zhang C, Zhou J, Xu K, Wang Q, Li Y, Zhang W. Microstructure and Mechanical Properties of Aluminum Alloy/Stainless Steel Dissimilar Ring Joint Welded by Inertia Friction Welding. Front Mater 2022; 8:813118. doi: 10.3389/fmats.2021.813118
20. Sakthivel P, Manobbala V, Manikandan T, Salik ZMA, Rajkamal G. Investigation on mechanical properties of dissimilar metals using MIG welding. Mater Today Proc 2020; 37:531–536. doi: 10.1016/j.matpr.2020.05.488
21. Shanjeevi C, Satish Kumar S, Sathiya P. Evaluation of mechanical and metallurgical properties of dissimilar materials by friction welding. Procedia Eng 2013; 64: 1514–1523. doi: 10.1016/j.proeng.2013.09.233
22. Sravanthi SS, Acharyya SG, Phani PP, Padmanabham G. Integrity of 5052 Al-mild steel dissimilar welds fabricated using MIG-brazing and cold metal transfer in nitric acid medium. J Mater Process Technol 2019; 268:97–106. doi: 10.1016/j.jmatprotec.2019.01.010
23. Sutrimo SA, Nugraha R, Koeshardono F, Suryadi A, Mulyana D, Casmita I. Effect of Heat Input Variations to the Mechanical Properties and Pitting Corrosion in the Dissimilar Stainless-Steel Welding. Int J Adv Sci Res Eng 2019; 5:116–123. doi: 10.31695/ijasre.2019.33541
24. Thirunavukarasu G, Chatterjee S, Kundu S. Scope for improved properties of dissimilar joints of ferrous and non-ferrous metals. Trans Nonferrous Met Soc China 2017; 27(7):1517–1529. doi: 10.1016/S1003-6326(17)60172-9
25. Touileb K, Djoudjou R, Hedhibi AC, Ouis A, Benselama A, Ibrahim A, Abdo HS, Samad UA. Comparative Microstructural, Mechanical and Corrosion Study between Dissimilar ATIG and Conventional TIG Weldments of 316L Stainless Steel and Mild Steel. Metals 2022; 12(4):635. doi: 10.3390/met12040635